Assessment of Solar PV Potential and Performance of a Household System in Durban North, Durban, South Africa

Williams S. Ebhota (ebhotawilliams1@gmail.com)
Durban University of Technology https://orcid.org/0000-0003-3099-3704
Pavel Y. Tabakov
Durban University of Technology

Research Article

Keywords: Renewable energy, Solar photovoltaic (PV), PV performance parameters, meteorological parameters, PV design and simulation applications, PV*SOL and Solargis

Posted Date: July 1st, 2021

DOI: https://doi.org/10.21203/rs.3.rs-644597/v1

Version of Record: A version of this preprint was published at Clean Technologies and Environmental Policy on November 24th, 2021. See the published version at https://doi.org/10.1007/s10098-021-02241-6.

Assessment of Solar PV Potential and Performance of a Household System in Durban North, Durban, South Africa

Williams S. Ebhota[1*] and Pavel Y. Tabakov[2]

[1,2]*Department of Mechanical Engineering, Institute for Systems Science, Durban University of Technology, Durban, South Africa.*

**Correspondence email: ebhotawilliams1@gmail.com*

Abstract

A rooftop solar photovoltaic (PV) system is an alternative electricity source that is increasingly being used for households. The potential of solar PV is location dependent that needs to be assessed before installation. This study focuses on the assessment of a solar PV potential of a site on coordinates -29.853762°, 031.00634°, at Glenmore Crescent, Durban North, South Africa. In addition, it evaluates the performance of a 6 kW installed capacity grid-connected rooftop solar PV system to supply electricity to a household. The results, obtained from PV design and simulation tools – PV*SOL, Solargis prospect and pvPlanner, were used to analyse and establish the site and PV system technical viability. The system's configuration is as follows: load profile - a 2-Person household with 2-children, energy consumption - 3500 kWh, system size - 6 kWp, installation type - roof mount, PV module type - c-Si - monocrystalline silicon, efficiency - 18.9%, orientation of PV modules -Azimuth 0° and Tilt 30°, inverter 95.9% (Euro efficiency), and no transformer. The results show: meteorological parameters - global horizontal irradiation (GHI) 1659.3 kWh/m^2, direct normal irradiation (DNI) 1610.6 kWh/m^2, air temperature 20.6 °C; performance parameters - annual PV energy 8639 kWh, Specific annual yield 1403 kWh/kWp, performance ratio (PR) 74.9%, avoided CO_2 emissions 5662 kg/year, and solar fraction 42.5 %. The analysis and benchmarking of the results show that the proposed solar PV system under the current conditions is technically viable for household electrification in Durban North, South Africa.

Keywords: Renewable energy**;** Solar photovoltaic (PV); PV performance parameters; meteorological parameters; PV design and simulation applications; PV*SOL and Solargis

1. Introduction

The deployment of solar photovoltaic (PV) systems is increasing due to the rising and uncontrollable fossil fuels prices, its environmental menace, and the continuous decline of solar PV components prices. In addition, it mitigates climate change consequences, promotes a decentralisation system, reduces dependence on energy imports, and extensive grid infrastructure. The continuous extensive use of fossil fuels is increasingly adding to the concentration of CO_2 in the atmosphere, which contributes to the global temperatures rise and environmental degradation (Almasoud & Gandayh, 2015). Energy conservation is receiving urgent attention due to the depletion of fossil fuels and the unabated price fluctuations. The use of fossil fuel contributes the highest share to CO_2; a by-product of fossil fuel combustion, emitted into the atmosphere (Nachmany et al., 2014). The sacrificing of the environment and human health for the energy required for socio-economic activities is presently attracting criticisms. However, this compromise has not bridged the gap of energy insufficiency in many developing countries. About 50% of the population in 41 countries in sub-Saharan Africa (SSA) have no adequate access to energy; 650 million people are expected not to have access to power by 2030 (IEA, 2017).

The present large economies are products of fossil fuels, such as natural gas, coal, and oil. These are unarguably effective economic boosters, but they leave behind negative environmental impacts and health consequences (Williams Saturday Ebhota, 2019; Williams S Ebhota & Tien-Chien Jen, 2018; Williams S. Ebhota & Tien-Chien Jen, 2018; W. S. Ebhota & Tabakov, 2018; Williams S. Ebhota & Tabakov, 2019). The consequential effects of the continuous use of these fuels to the biosphere (Aljazeera, 2019; FloodList, 2019a, 2019b) are evidenced in the increasing climate change triggered events. Some of these events are the unceasing rise in temperatures, droughts, flood, cyclone, storms and ice melts, and migration. Several efforts to check the aforementioned energy issues have been advanced, and these include measures to reduce energy consumption, maximization of the use of renewable energy (RE), use of hybrid renewable energy system (HRES) (Rinaldi, Moghaddampoor, Najafi, & Marchesi, 2021), digitalization and decentralization of energy system (DCES), and the smart grid.

1.1. The need for alternative energy

The decision by the United Nations (UN) to cut down the global consumption of fossil fuel, to reduce the effect of CO_2 emissions was well-received globally (UN, 2015). However, there is a need to develop alternative energy sources to replace fossil fuel; since energy is what powers socio-economic growth. These alternatives are expected to be clean, reliable, adequate, and affordable energy. Sustainable energy transition will simply be fiction or a mirage without alternative energy to replace fossil fuel (W. S. Ebhota, Eloka-Eboka, & Inambao, 2014; Williams S. Ebhota & Inambao, 2015; Williams S Ebhota & Inambao, 2017). Subsequently, the contemporary

questions surrounding energy are centred on how to harness RE resources; raise the efficiency of supply and end-use; reduce CO_2 emissions originating from energy generation and consumption; and provide clean energy for all. This implies that much advancement has to be made to improve and facilitate RE deployment. Renewable energy technologies such as solar, biofuels, hydro, geothermal, tidal, and wind are currently receiving massive interest in terms of deployment, investment, and research and development. In addition, nuclear energy has also been described as reliable, safe, clean, compact, competitive, and practically inexhaustible (Eiden, 2014). However, because of the perceived side effects, many countries are sceptical about the use of energy although nuclear has enormous energy required for electricity. The study aims to facilitate the generation of clean electricity through the deployment of solar PV for the reduction of fossil fuel consumption.

1.2. Solar energy

Amongst the three most harnessed RE resources (solar, small hydropower, and wind), solar photovoltaic is the most deployed. This is mainly because of its widespread availability coupled with the continuous price decline of PV components, easy installation, and low maintenance cost. Solar energy is regional dependent and the annual direct solar irradiation in some regions exceeds 300 Watt per square meter (W/m^2). A study observed that many of the countries that are likely to experience a rapid increase in urbanisation are in solar-rich regions, such as Singapore, Nigeria, Spain, Australia, India, and South Africa ("World Energy Council. (2013, 15/01/2018). World Energy Resources: Solar "). This gives solar PV systems the greatest potential for wider utilisation in SSA. Singapore is already exploiting the PV system, and have planned to raise solar power through a roadmap that adopts two scenarios - a “baseline” (BAS) scenario and an “accelerated” (ACC) scenario (Roadmap, 2020). The targets of these scenarios are BAS - 1 GWp and 2.5 GWp by 2030 and 2050, respectively; ACC - 2.5 GWp and 5 GWp by 2030 and 2050, respectively. The success of this plan will save the yearly CO_2 emissions of about 1.6 million tonnes (Mt) and 3.4 Mt by 2030 and 2050, respectively. The realisation of the significance of massive deployment of the different scales of solar PV systems in SSA will help to address the frequent blackouts and inadequate power supply considerably. At the same time, it would facilitate the building of a sustainable energy system in the end, which will reduce CO_2 emissions (Njoku & Omeke, 2020).

Despite the successes recorded in solar efficiency, structure, and cost, the efficiency of multi-crystalline silicon photovoltaic (PV) cell is hovering around 10% to 17% (Kammen & Sunter). Recently, PV laboratory studies have reported efficiency of over 40%, using concentrated multi-junction cells (NREL, 2016). Researches are still ongoing to further improve the PV panel conversion performance and cost decline. Hence, this study assesses the solar PV potential of Glenmore Crescent, Berea, KwaZulu-Natal in South Africa and use the information to design a solar PV system for the location. The objectives of the study include discussion and analysis of site-specific meteorological factors, and PV performance parameters; comparison of the annual energy yield and prediction of the performance of 6 kWp grid-connected rooftop solar power plant.

2. Background of study

2.1. Solar resource basics and modelling solar radiation

Solar radiation is used to assess the potential power levels that can be generated from photovoltaic cells, and necessary for determining cooling loads for buildings. Hence, accurate quantification of solar radiation is required for various PV system applications, such as agricultural and water resource planning, management, and the design of irrigation systems. Additionally, solar radiation is the most basic and reliable renewable and clean energy source in nature that can play an alternative role to fossil fuels. Therefore, the knowledge of solar radiation is essential for the optimal design and evaluation of solar energy applications, such as photovoltaic and solar-thermal systems. Solar radiation takes a reasonable time before it reaches the Earth’s surface, causing it to have various extra-terrestrial interactions with the atmosphere and surfaces of objects along its path. The amount of solar radiation per unit of horizontal area for a given locality is called, insolation, it originates from the sun, and depends mainly on the distance between the earth and sun, and solar zenith angle. Insolation can also be altered by the atmosphere, topography and surface features, as it travels down the earth. At the earth's surface, it forms three radiation components, as shown in Fig 1 - direct, diffuse, and reflected radiations − the direct radiation makes a direct line from the sun as it is intercepted by the earth unobstructed; the diffuse radiation is dispersed by atmospheric constituents, such as dust and clouds as it travels through them; and the reflected radiation hits on surface features along its path and gets reflected. The summation of these three radiation components is called global or total solar radiation.

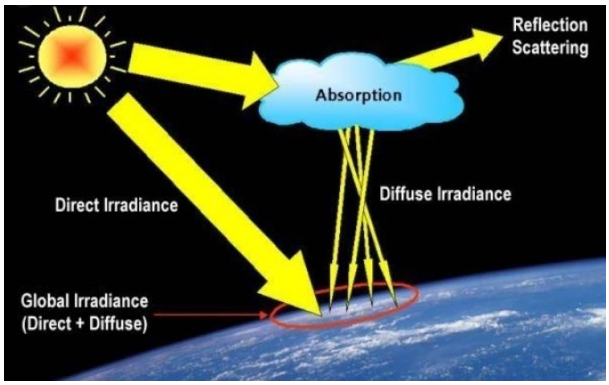

Fig 1: Components of total/global radiation (direct, diffused, and reflected radiations) (Cotfas, N/A)

Amongst these three components, direct radiation is the largest component, followed by diffuse radiation while the reflected radiation constitutes the least proportion, except for locations surrounded by highly reflective surfaces, such as snow-covered areas. The point locations or entire geographic area’s radiation can be estimated

using solar radiation tools and this involves the following four steps (Alamoud, 2000; Cioban, Criveanu, Matei, Pop, & Rotaru, 2013; Rich, Dubayah, Hetrick, & Saving, 1994):

i. The computation of an upward-looking hemispherical viewshed based on topography.
ii. Estimation of direct radiation by overlaying the viewshed on a direct sun map.
iii. Estimation of diffuse radiation by overlaying the view-shed on a diffuse sky map

This process can be repeated for every location of interest to create an insolation map.

2.2. Mathematical calculation of insolation

The solar radiation analysis tools compute insolation throughout a landscape or for particular locations, centre on techniques from the hemispherical view-shed algorithm created by Rich et al. (Fu & Rich, 2002; Rich et al., 1994). The total radiation is computed for a specific location and is given as global radiation. The computation of direct, diffuse, and global insolation is replicated for every featured location on the topographic surface, creating insolation maps for the total geographical area.

Direct Normal Irradiation/Irradiance (DNI) is the element that deals with the photovoltaic concentration technology (concentrated photovoltaic, CPV) and thermal (concentrating solar power, CSP).

Global Horizontal Irradiation/Irradiance (GHI) is the summation of direct and diffuse radiation collected on a horizontal plane. GHI is used as the basis for climatic zones radiation comparison and is an essential parameter for computing radiation on a tilted plane.

Global Tilted Irradiation/Irradiance (GTI), or total radiation collected on a surface with set tilt and azimuth angles, fixed or sun-tracking is the summation of the direct, scattered, and reflected radiation. It is occasionally affected by shadow and is used for PV applications.

2.2.1. Global radiation calculation

The estimated of global radiation ($Global_{tot}$) is:

$$Global_{tot} = Dir_{tot} + Dif_{tot} \quad (1)$$

Where Dir_{tot} and Dif_{tot} are direct and diffuse radiation of all sun map and sky map sectors, respectively.

$$Dir_{tot} = \Sigma Dir_{\theta,\alpha} \quad (2)$$

$$Dir_{\theta,\alpha} = S_{Const} * \beta^{m(\theta)} * SunDur_{\theta,\alpha} * SunGap_{\theta,\alpha} * cos\left(AngIn_{\theta,\alpha}\right) \quad (3)$$

Where $Dir_{\theta,\alpha}$ is the direct insolation from the sun map sector $(Dir_{\theta,\alpha})$ with a centroid at zenith angle (θ) and azimuth angle (α); S_{Const} is the solar constant, and 1367 W/m^2 is usually used in the analysis; β is the transmissivity of the atmosphere; $m(\theta)$ is the relative optical path length; $SunDur_{\theta,\alpha}$ is the time duration represented by the sky sector; $SunGap\theta,\alpha$ is the gap fraction for the sun map sector; $AngIn\theta,\alpha$ is the angle of incidence between the centroid of the sky sector and the axis normal to the surface.

Relative optical length, $m(\theta)$, is function of solar zenith angle (θ) and elevation above sea level. For zenith angles less than 80°, relative optical length, $m(\theta)$:

$$m(\theta) = EXP\left(-0.000118 * Elev - 1.638 * 10^{-9} * Elev^2\right) / cos(\theta) \quad (4)$$

Angle of incidence $(AngInSky_{\theta,\alpha})$:

$$AngIn_{\theta,\alpha} = acos\left(Cos(\theta) * Cos(G_z) + Sin(\theta) * Sin(G_z) * Cos(\alpha - G_a)\right) \quad (5)$$

Where G_z is the surface zenith angle, and G_a is the surface azimuth angle

2.2.2. Computation of diffuse radiation

The diffuse radiation at its centroid (D_{if}) is estimated, integrated over the time interval, and corrected by the gap fraction and angle of incidence utilizing this expression in (6):

$$Dif_{\theta,\alpha} = R_{glb} * P_{dif} * Dur * SkyGap_{\theta,\alpha} * Weight_{\theta,\alpha} * cos\left(AngIn_{\theta,\alpha}\right) \quad (6)$$

Where R_{glb} is the global normal radiation; P_{dif} is the proportion of the diffused global normal radiation flux (it is usually estimated 0.2 for very clear sky conditions and 0.7 for very cloudy sky conditions); D_{ur} is the time interval for analysis; $SkyGap_{\theta,\alpha}$ is the gap fraction for the sky sector (proportion of visible sky); $Weight_{\theta,\alpha}$ is the proportion of diffuse radiation starting from a given sky sector relative to all sectors; $AngIn_{\theta,\alpha}$ is the angle of incidence between the centroid of the sky sector and the intercepting surface.

The global normal radiation (R_{glb}) can be computed by summing up the direct radiation from every sector, without correction for angle of incidence, then correcting the proportion of direct radiation, which equals 1-P_{dif}:

$$R_{glb} = \left(S_{Const}\Sigma\left(\beta^{m(\theta)}\right)\right) / \left(1 - P_{dif}\right) \quad (7)$$

$$Weight_{\theta,\alpha} = \left(cos\theta_2 - cos\theta_1\right) / Div_{azi} \quad (8)$$

Where θ_1 and θ_2 are the bounding zenith angles of the sky sector; Div_{azi} is the number of azimuthal divisions in the sky map.

For the standard overcast sky model, $Weight_{\theta,\alpha}$ is computed as follows:

$$Weight_{\theta,\alpha} = \left(2cos\theta_2 + cos2\theta_2 - 2cos\theta_1 - cos2\theta_1\right) / 4 * Div_{azi} \quad (9)$$

Total diffuse solar radiation for the location (Dif_{tot}) is computed as the sum of the diffused solar radiation *(Dif)* from all the sky map sectors:

$$Dif_{tot} = \Sigma\, Dif_{\theta,\alpha} \quad \text{_____ (10)}$$

2.3. Solar PV system design and simulation applications

Many reliable and innovative software applications have been developed to carry out solar PV assessment, system design, costing, energy generation prediction, and operation activities. Other uses are obtaining PV site location and meteorological information, assessing the site's solar PV potential, and conducting system design, PV panel degradation assessment, and financial analysis. The impacts of the sun on a geographic area of a given period can be mapped and analysed using solar radiation analysis tools that exploit two methods:

i. Calculation of insolation across an entire landscape, in a repeated manner for each location in the input topographic surface, using area solar radiation tool landscape.

ii. Calculation of the amount of radiant energy for a specified location, using the point's solar radiation tool.

In addition, they are used by solar installers for system design for stand-alone/off-grid, grid-connected, and hybrid systems for industrial plants, commercial, and residential buildings (Li, 2021). Some of these applications and their uses are presented in Table 1.

Table 1: Software applications used for solar PV systems performance analysis (Dondariya et al., 2018; Fuzen, 2021; Khatib, Mohamed, & Sopian, 2012)

Software	Software specifications	Inputs required
PV*SOL	It is applied for the Planning and simulation of a site-specific solar PV system.	Location Coordinates, meteorological data, system and auxiliary devices requirements
SolarGIS	A satellite map-supported online simulation tool for site assessment, planning and optimization of solar PV systems, and comparing energy harvest from various PV technologies.	Type of PV technologies, local coordinates, AC/DC losses, load demand, cable sizing.
PVGIS	An open-source research tool for performance assessment of PV technology in geographical regions and as a support system for policymaking in the European union	Total irradiance, Monthly values of atmospheric conditions, the mounting position
SISIFO	An open web service software for simulation of PV systems	Location of the system, the solar resource data, technical characteristic of the system and optionally system economics.
PVsys	A software application for the study, sizing, and data analysis of complete PV systems. The PV systems include stand-alone, grid-connected, pumping and DC-grid. The application has extensive metrological and PV systems components databases, as well as general solar energy tools	conditions and parameters specific to a project

3. Methodology

The study involves the assessment of solar PV potential of Glenmore Crescent, Durban North, South Africa; estimation of the electricity generation capacity of the location; and model solar PV system. The study will exploit the geospatial technology of two PV software applications, PV*SOL and Solargis, to evaluate and present solar resource information, PV system design model, simulation, and optimization results. The software applications are supported with satellite-derived annual global solar radiation and temperature data. The assessment will be used to define the amount and pattern of solar insolation and the capacity of PV power that can be generated by the solar resource. This information will be inputted in the modelling of solar PV system for the generation of electricity with net-zero or sub-zero CO_2 emissions. The schematic diagram in Fig 2 represents the flowchart of the methodology employed in this study.

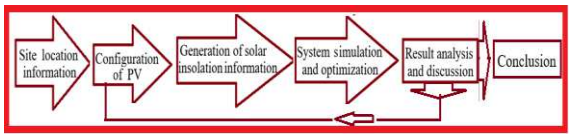

Fig 2: Schematic of the methodology flowchart

3.1. Location information and system description

Detailed information of the site location is a requirement for an accurate solar PV potential estimation since the performance of the PV system depends on site-specific meteorological factors. These factors are wind speed, solar irradiance characteristics, and ambient temperature. Other determinants are installation site factors, which include dust, pollution level, latitude, orientation, and tree cover. The site is located in a residential area and a section of the site, as obtained from Google Map, is shown in Fig 3.

Fig 3: A section of Glenmore Crescent, Durban North, South Africa

For this study, a hypothetical household building was selected as a site, at a latitude of 29.800955°, the longitude of 31.0327245° in Glenmore Crescent, Durban North, South Africa. Other information on the selected site is presented in Table 2.

Table 2: the site location and the system information

Site location information	
Project name	Durban North
Address	Glenmore Crescent, Durban North, South Africa
Geographical coordinates (°)	-29.800955, 31.0327245
Time zone	UTC+02, Africa/Johannesburg [SAST]
Elevation (m)	48
Land cover	Urban areas
Population density (inh./km^2)	2892
Terrain azimuth (°)	118
Terrain slope (°)	3
Annual air temperature at 2 m (°C)	20.9

Generally, the grid-connected PV system is made up of solar PV panel arrays, a solar inverter, electrical panel, array mounting racks, cabling, meters, combiner box, surge protection, disconnects (array DC disconnect, inverter DC disconnect, inverter AC disconnect, exterior AC disconnect), and grounding equipment other electrical accessories, as shown in Fig 4.

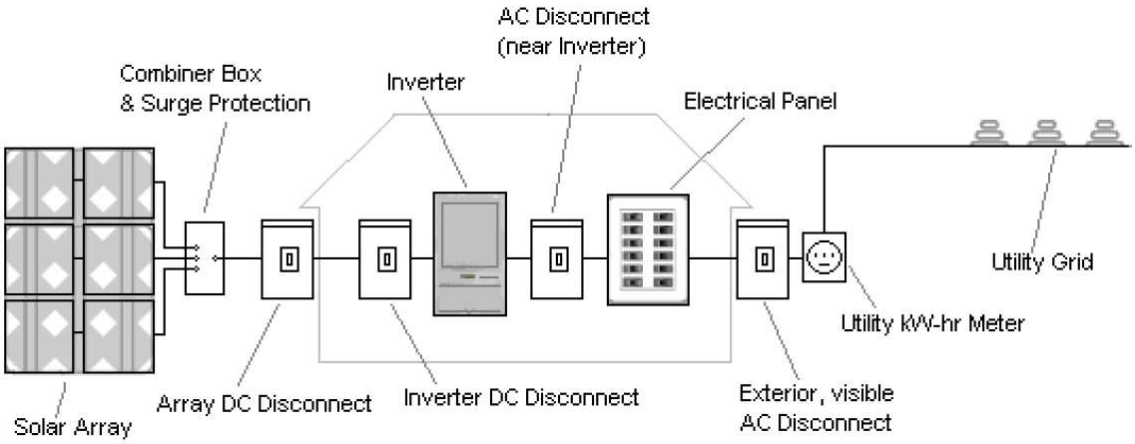

Fig 4: Components of the grid-connected PV system (Roos, Nelson, & Brockman, 2009)

3.2. Simulation of grid-connected PV system

The selection of the load profile, PV module, and installation types will be carried out using solar PV potential evaluator and design applications. Based on inputs optimisation considerations, the PV*SOL and Solargis software applications will be used to evaluate various parameters of a solar PV system, such as the daily, monthly, and yearly irradiations, terrain horizon and day length, energy production, annual yield, and total system losses. In addition, a tabular comparative analysis of some critical solar system parameters overview will be presented.

4. Simulation results and discussion

This section presents a detailed description of the load profile, configuration of the PV system, and the inputted parameters. It also includes simulation results presentation, analysis, and discussion of solar irradiations, energy production, annual yield, and total system losses.

4.1. The description of the system

The installation type used in this study is a rooftop mount, meaning that the 6 kW_p-installed capacity of the PV system was hypothetically mounted on a tilted roof of a residential building. The Azimuth and angle of tilt of the PV panels are harmonised such that the panels do not overlap or shade each other. The mounting of PV panels on rails that are attached to a tilted roof gives room for backside ventilation. A low-voltage grid connection, which is in a parallel circuit connection, through an inverter without storage is suitable for this type of PV system. Monocrystalline PV cell material was selected because of the quest for higher efficiency and the system is on a fixed stand type that can adequately power a household of a small family. Details of other inputs used in this study are presented in Table 3.

Table 3: System information

Load profile	2-Person household with 2-children
Energy consumption (kWh)	3500
System size (kWp)	Installed capacity: 6
Installation type	Roof mount
PV module type (%)	c-Si - crystalline silicon (mono), efficiency 18.9
Geometry of PV modules (°)	Azimuth: 0; Tilt: 30
Inverter type (%)	Inverter 95.9 (Euro efficiency)
Transformer type	No transformer
Snow and soiling losses at PV modules (%)	Monthly soiling losses up to 4.5; Monthly snow losses up to 0.0
Cabling losses (%)	DC cabling 1; DC mismatch 0.8; AC cabling 0.2
Albedo	20
System availability (%)	97

4.1.1. The potential solar resource - solar irradiation

Solar insolation fuels the PV power system, hence, is the most significant project-specific meteorological parameter that defines or boosts solar electricity generation. Solar irradiation was used professionally to evaluate the energy yield of a PV system site at Glenmore Crescent, Durban North. The estimates of solar monthly and yearly variations of GHI, DNI, and DIF of the

selected site, as obtained from Solargis Prospect, are depicted in Fig 5 (a) and (b), respectively. Durban North has GHI relatively high in seven months - from January to March, and September to December and low for four months – April to August, as shown in Fig 5(a).

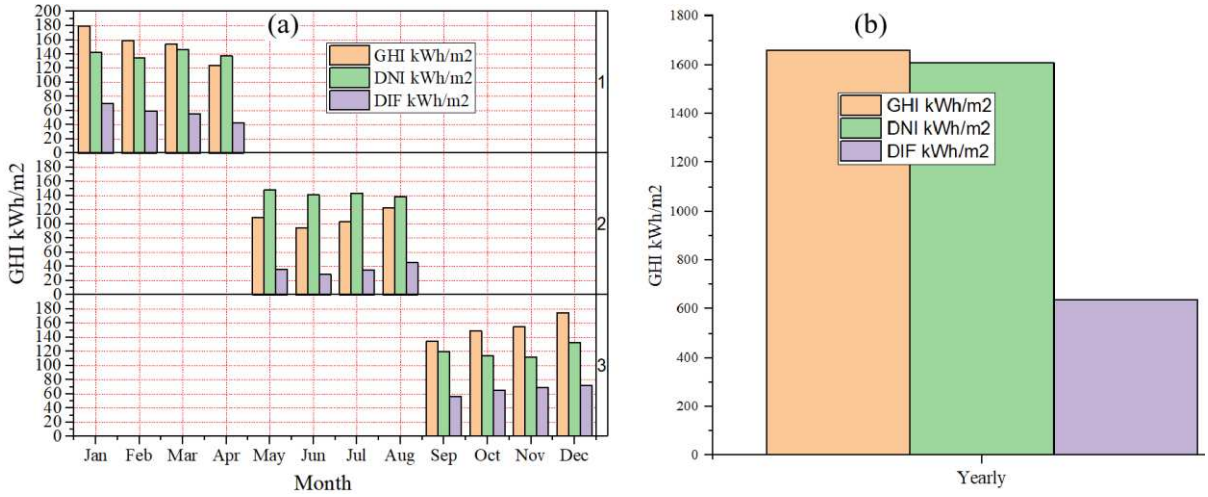

Fig 5: The estimates of (a) solar monthly and (b) yearly variations of GHI, DNI, and DIF of Durban North

The highest irradiation of the site under consideration is in January; the results from Solargis Prospect and PV*SOL show 180 kWh/m^2 at 24 °C and 190 kWh/m^2 at 21 °C, respectively, as shown in Fig 6 (a) and (b). The range of solar insolation received by the site throughout the year is from 95 to 190 kWh/m^2. The pattern of irradiance obtained, further strengthened the assertion that solar energy significantly depends on seasonal variation across the year.

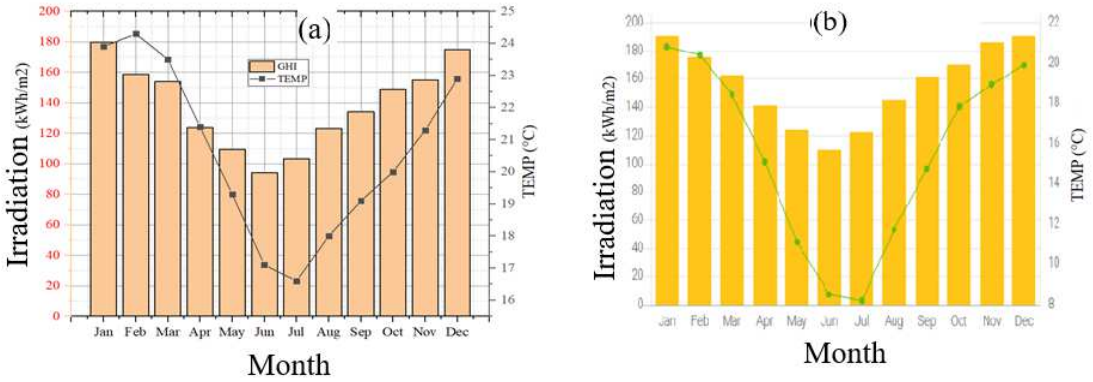

Fig 6: Monthly irradiation and temperature data at Durban North, South Africa obtained from (a) Solargis; and (b) PV*SOL

4.1.2. Terrain horizon and day length

The length of a day is determined by the following factors - geographical latitude of the location, altitude of the sun, hour angle, and the sun declination angle. Fig 7(a) presents the horizon and sun path over a year in Durban North (the module horizon, terrain horizon, and active area with civil and solar time), which may have a shading effect on solar radiation. The change of day length and minimum zenith angle during a year are presented in Fig 7(b). The local day length (the time when the Sun is above the horizon) is shorter compared to the astronomical day length if obstructed by a higher terrain horizon.

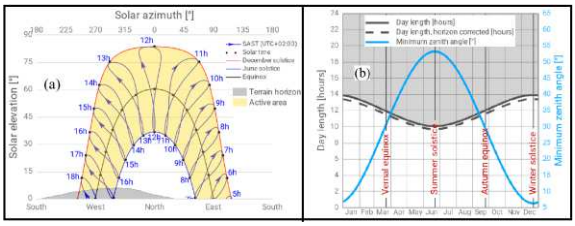

Fig 7: (a) Path of the sun over a year in Surabaya; (b) Day length and solar zenith angle

4.2. Performance parameters

The sustenance of the ongoing development of the solar PV industry depends critically on the accurate PV system performance. The performance parameters are used to make comparisons of systems with different geographic locations, design, and/or technology, and to allow operational problems detection. These parameters, which include performance ratio (PR), reference yield, final PV system yield, and Photovoltaics for utility-scale applications (PVUSA) rating, define the overall system performance concerning the solar resource, energy production, and total system losses effect (Marion et al., 2005). One of the most significant variables for estimating the efficiency of a PV plant is PV.

4.2.1. Performance ratio (PR)

The performance ratio is the ratio of the actual energy output and the possible theoretical energy output. It is

mainly independent of the positioning of a PV plant and the incident solar irradiation on the PV plant. It is a measure of a PV system performance, taking into account meteorological factors, such as irradiation, climate changes, relative humidity (RH), and temperature. Hence, the PR can be used to compare PV plants supplying the grid at various locations all over the world.

The ratio between specific alternating current (AC) electricity output of a PV system and global tilted irradiation (GTI) obtained by the surface of a PV array, is termed as performance ratio (PR).

$$PR = \frac{PV_{OUTspecific}}{GTI} \quad (12)$$

Also,

$$PR = Y_f / Y_r = \left(E_{out}/P_o\right) \Big/ \left(H_i/G_{i,ref}\right) \quad (13)$$

Where $PV_{OUTspecific}$ is the specific photovoltaic power output (kWh/kWp), G_i is the sum of direct, diffuse, and ground-reflected irradiance incident upon an inclined surface parallel to the plane of the modules in the PV array, H_i is the in-plane irradiation kWh/m^2, E_{out} is the Energy output from PV system (AC), (kWh); P_o, is the array power rating, AC, (kW).

The computation and report of PR are based on monthly or yearly output, although it can be calculated for smaller intervals, such as daily or weekly. This may be used to identify the occurrences of component failures. Because of losses due to PV module temperature, the values of PR in the winter are greater than in the summer, which usually falls within the range of 0.6 to 0.8. The maximum energy production is 1100 kWh in August, while the minimum is 810 kWh in February, as shown in Fig 8. The reasons behind the high yield in August are the longest day of sunshine and low ambient temperature. The cloudy or rainy season is responsible for the low yield in February. Similarly, heavy electrical load, such as water geyser, and room heater connected to the system during winter accounts for the high-energy consumption (300 kWh) in July and August.

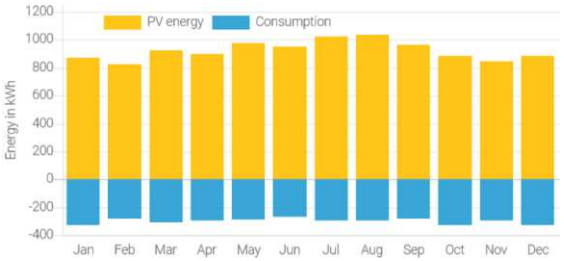

Fig 8: Annual energy production and consumption

For the small household, the projected total energy consumption from the software is 3500 kWh. The PV system supplied 1502 kWh, about 43%, and the remaining energy consumption covered by the grid is 1998 kWh. The total annual energy produced from solar PV and consumed are 10854 kWh and 1502 kWh, respectively. This means that 9,082 kWh (about 86% of the energy generated) will be connected to the grid, as shown in Fig 9.

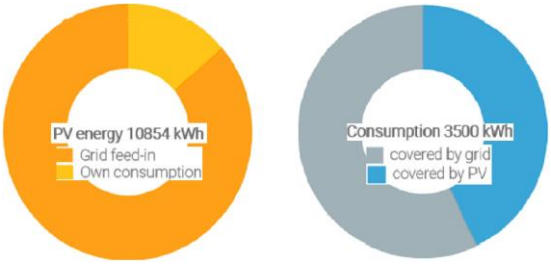

Fig 9. Energy feed-in grid and energy consumption covered by PV and grid

4.3. Effects of relative humidity, temperature, and wind speed

The power output of a PV system is significantly affected by the minimum and maximum ambient temperatures (Temp), wind speed (WS), and relative humidity (RH) (Park, Oh, & Kim, 2013; Shrestha, Thapa, & Gautam, 2019). The rise of cells temperature coupled with mismatch losses, dust accumulation, power-point errors, and shading, account for array capture losses (L_c), which is the difference between the reference (Y_R) yield an array yield (Y_F) (Atsu, Seres, & Farkas, 2021; Marion et al., 2005; Shiva Kumar & Sudhakar, 2015). Where Y_F is also known as the final yield of the system. Mathematically, the array capture losses is computed using this expression:

$$L_c = Y_R - Y_F \quad (11)$$

High humidity, Temp, and WS affect the performance of the PV module adversely. The humidity condenses and creates a deposit on the PV panel at the night and this cause greater deflection of irradiance during the day. The curves of RH, temperature and WS for the Durban North site showed a similar pattern, as presented in Fig 10.

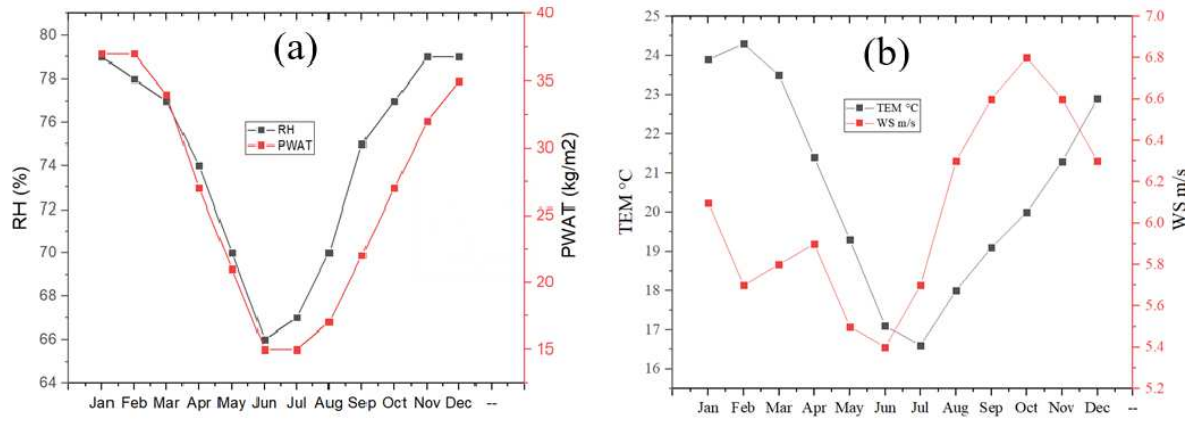

Fig 10: RH, Temp, and WS components of meteorological parameters

The testing and rating of solar panels are usually carried out at about 25 °C and are expected to perform optimally between 15 °C and 35 °C. However, during the summer, the temperature of solar panels in some areas may be as high as 65 °C (BostonSolar, 2021). According to the meteorological information obtained from Solargis, the annual average temperature of Durban North is 20.6 °C while the lowest (16.6 °C) and highest (24.3 °C) temperatures of Durban North were recorded in July and February, respectively. Further evaluation and analysis of the project-specific meteorological parameters, as presented in Fig 11, shows that the relation between PR and RH; and PR and temperature are both inverses:

i. The highest PR corresponds to the lowest temperature value. This means that the PV system produces more energy at low temperature. It implies that the solar PV system is more efficient at low temperature.

ii. The months (June and July) are of a very high PR, which corresponds to the months of a relatively low RH value. This means that the PV system produces more energy when humidity is low. Low humidity causes little limitation to electricity production by the solar PV system.

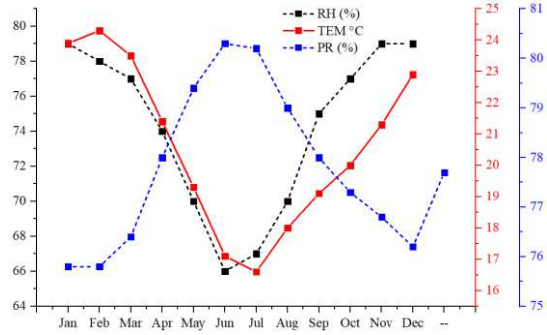

Fig 11: The graph of RH, Temp and PR

The efficiency of the PV module is highly affected by the sensitivity of the Si-based PV module to cell temperature. Consequently, there is a notable solar PV system efficiency loss in locations with long hot seasons, due to high temperatures. The negative effects of elevated temperatures on PV system can be minimized in many ways. These include - leaving few millimetres between the panel and the roof to allow convectional airflow to cool the panels; use of light-coloured materials to construct panels to reduce heat absorption; and keep components, such as inverters and combiners under a shaded area behind the array. The influence and relation of other solar PV parameters are presented in Fig 12.

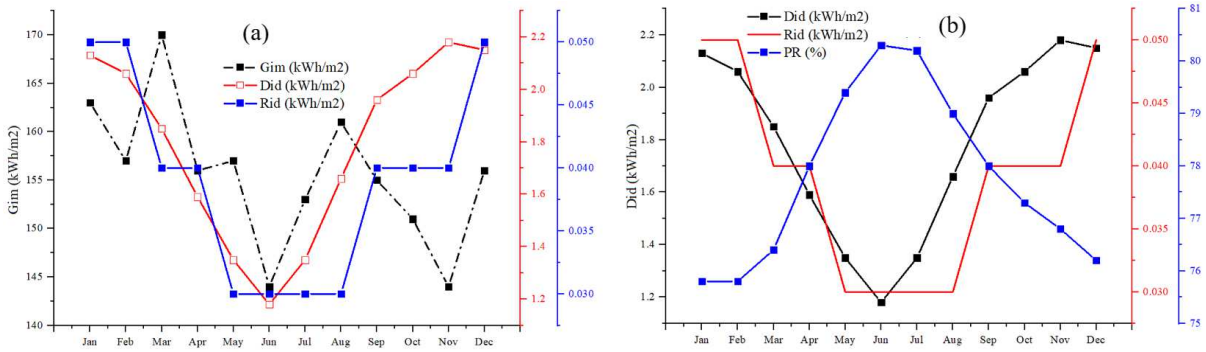

Fig 12: Effect of humidity on irradiance (a) reflected irradiance; (b) reflected irradiance and PR

Where Gi_m is the monthly sum of global irradiation (kWh/m^2), Gi_d is the daily sum of global irradiation (kWh/m^2), Di_d is the daily sum of diffuse irradiation (kWh/m^2) and Ri_d is the daily sum of reflected irradiation (kWh/m^2)

4.4. Other PV performance determinants

Many parameters, aside from the ones discussed above, are used to determine the potential of PV and the level of performance of a location and system, respectively. Some of these are the ratio of diffuse horizontal irradiation to global horizontal irradiation (D2G); Fraction of solar irradiance reflected by surface, the ratio of upwelling to

downwelling (GHI) radiative fluxes at the surface, known as surface albedo (ALB). Others are soiling losses and snow losses; the quantification of energy demand needed to cool a building, called cooling degree-days (CDD); and presented in Table 4.

Table 4: PV performance determinants

Month	Jan	Feb	Mar	Apr	May	Jun	Jul	Aug	Sep	Oct	Nov	Dec	Yearly
D2G	0.393	0.372	0.36	0.349	0.325	0.312	0.337	0.37	0.417	0.438	0.447	0.415	0.384
CDD degree days	179	175	172	106	69	37	29	42	44	66	94	143	1155
HDD degree days	0	0	0	0	3	19	32	20	11	1	0	0	87
Soiling losses %	4.5	4.5	4.5	4.5	4.5	4.5	4.5	4.5	4.5	4.5	4.5	4.5	
Snow losses %	0.0	0.0	0.0	0.0	0.0	0.0	0.0	0.0	0.0	0.0	0.0	0.0	

Durban North experiences temperature between 16.6 °C and 24.3 °C, rainfall, spectacular thunderstorms, and high humidity that can make muggy days during summer, usually from October to March. These conditions hinder solar PV production performance and that is why the PR in these months are relatively low. In winter (June-August), the condition is different, as the temperature is between 0 °C and 20 °C and July is the sunniest month with an average temperature of 22 °C. The various weather conditions across the year are shown in Fig 13(a). The southern position in the hemisphere accounts for the times of sunrise and sunset in South Africa. Part of autumn (May) and winter months (June-August) have the longest days, while the summer months (December-February) have the shortest days (Worlddata.info, 2021). The Durban average monthly hours of sunshine is represented in Fig 13(b).

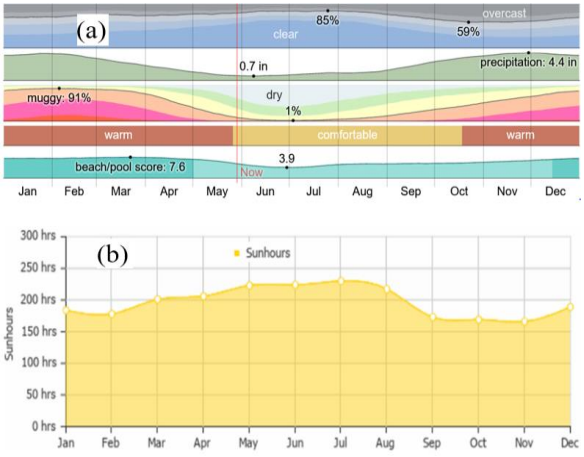

Fig 13: Durban North average monthly hours of sunshine (Weather&Climate, 2021)

Solar PV performance: Energy conversion and system losses

The evaluation of the long-term average performance ratio (PR) is important and required for a start-up production of a PV system. The overview of the theoretical yearly specific estimate of solar electricity generation by a PV system, without the long-term ageing

and performance degradation of PV modules and other system components reflection, are presented in Table 5 and Fig 8.

Table 5: System losses and performance ratio

Energy conversion step	Energy output kWh/kWp	Energy loss kWh/kWp	Performance ratio %	Partial %	Cumul. %
Global in-plane irradiation (input)	1873	-	-	100.0	100.0
Global irradiation reduced by terrain shading	1865	-7	-0.4	99.6	99.6
Global irradiation reduced by reflectivity	1817	-48	-2.6	97.4	97.1
Conversion to DC in the modules	1594	-224	-12.3	87.7	85.1
Other DC losses	1506	-88	-5.5	94.5	80.4
Inverters (DC/AC conversion)	1469	-38	-2.5	97.5	78.4
Transformer and AC cabling losses	1447	-22	-1.5	98.5	77.3
Reduced availability	1403	-43	-3.0	97.0	74.9
Total system performance	**1403**	**-469**	**-25.1**	**-**	**74.9**

The estimation of the energy conversion and losses steps using Solargis PVplanner can be categorized into two components - losses numerically modelled by pvPlanner and losses that are assessed by the user. The integration of these components gives the theoretical losses due to energy conversion in the PV power system, as depicted in Fig 14.

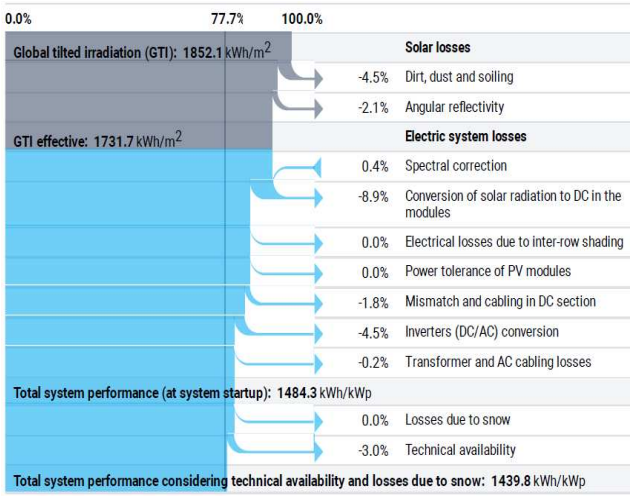

Fig 14: The theoretical losses due to energy conversion in the PV power system

Performance comparison

The summary of the technical performance simulation of the solar PV system obtained from the three PV software applications is reported in Table 6. The results obtained from software applications, PV*SOL, Solargis Prospect, and PVplanner, were similar. The outputs from Solargis Prospect and PVplanner were closer, while PV*SOL energy output deviates much more, compared to the other two. Solargis Prospect and PVplanner reported March as the month with the highest energy output while PV*SOL shows maximum energy output in August. The rise in temperature causes a decrease in solar PV output; hence, the output in March should be less, while the moderate temperature in August allows energy conversion from the solar PV system. This was observed in PV*SOL energy output only and the PR pattern outputs of both Solargis and PVplanner applications. The PR obtained from PV*SOL is significantly higher than Solargis software applications.

Table 6: summary of results obtained from PV*SOL, and SolarGIS Prospect and PVplanner

PV software application	**PV*SOL**	**SolarGIS-Prospect**	**SolarGIS-PVplanner**
Meteorological parameter			
Global horizontal irradiation (kWh/m^2)	1877	1659.3	1865
Direct normal irradiation (kWh/m^2)		1610.6	
Diffuse horizontal irradiation (kWh/m^2)		636.6	
Air temperature (°C)	15.5	20.6	20.9
Performance parameter			
Annual PV energy (kWh)	10583	8639	8419
Spec. annual yield (kWh/kWp)	1763.88	1439.8	1403
Month with max energy output	August	March	March
Average PR, (%)	88.89	77.7	74.9
Month with max PR (%)			
Avoided CO_2 emissions (kg/year)	5662		
Solar fraction (%)	42.5		

Conclusion

A monocrystalline solar PV system was used to determine the technical performance parameters of a 6 kW installed capacity grid-connected rooftop solar PV system to supply electricity to a household. The parameters include energy yield assessment, energy consumption, electricity feed-Ingrid, and performance ratio. The study was performed using PV*SOL, SolarGIS-Prospect, and SolarGIS-pvPlanner. It was observed that there were variations in the predicted values of annual energy production, PR, Specific annual energy yield, and energy yield. These variations were attributed to the difference in model equations and source of climate data amongst the simulation software applications. However, the absence of checked irradiance data and PV power output restrains the proof of the results. The study presents some valuable perceptions into the rooftop PV system to meet the normal household's energy needs, irrespective of the noted shortcomings. The key points obtained from the simulation results are as follows:

i. The reported annual energy yield of 1403 kWh/kWp, shows that the monocrystalline PV module rooftop grid-connected system installations in Durban North of South Africa are technically viable green energy alternative for residential areas, government buildings, business centres, etc.

ii. Depending on the available rooftop area, the PV energy production performance is good with the scope of capacity scale up above 6 kWp in the Durban North region.

iii. The annual energy production of 8419 kWh was reported and about 86% of this was fed into the grid.

iv. The solar PV system PR of 74.9% obtained is satisfactory for installation and commissioning

v. By using the proposed PV system, an estimated 43% reduction of the annual energy requirement from the electrical grid was obtained.

vi. Comparatively, PV*SOL exhibits easy, fast, and most reliable trends as a simulation tool for the solar PV system.

vii. The proposed grid-connected rooftop PV system in Durban North is feasible as the results show technical viability, with the benefits of clean energy provision, CO_2 emission reduction, and energy savings.

Acknowledgement

The authors hereby acknowledge the Research and Postgraduate Support Directorate, Institute for Systems Science, and the Management of Durban University of Technology, South Africa, for their continuous support.

Conflict of interest statement

The authors declare that there is no conflict of interest

References

Alamoud, A. R. M. (2000). Characterization and Assessment of Spectral Solar Irradiance in Riyadh, Saudi Arabia. *Journal of King Saud University - Engineering Sciences, 12*(2), 245-254. doi:https://doi.org/10.1016/S1018-3639(18)30717-7

Aljazeera. (2019). East Africa struggles with heavy rains as thousands displaced. Retrieved from https://www.aljazeera.com/news/2019/11/east-africa-struggles-heavy-rains-thousands-displaced-191129061914721.html

Almasoud, A. H., & Gandayh, H. M. (2015). Future of solar energy in Saudi Arabia. *Journal of King Saud University - Engineering Sciences, 27*(2), 153-157. doi:https://doi.org/10.1016/j.jksues.2014.03.007

Atsu, D., Seres, I., & Farkas, I. (2021). The state of solar PV and performance analysis of different PV technologies grid-connected installations in Hungary. *Renewable and Sustainable Energy*

Reviews, 141, 110808. doi:https://doi.org/10.1016/j.rser.2021.110808

BostonSolar (Cartographer). (2021). How do temperature and shade affect solar panel efficiency? Retrieved from https://www.bostonsolar.us/solar-blog-resource-center/blog/how-do-temperature-and-shade-affect-solar-panel-efficiency/

Cioban, A., Criveanu, H., Matei, F., Pop, I., & Rotaru, A. (2013). Aspects of Solar Radiation Analysis using ArcGis. *Bulletin UASVM Horticulture, 70*(2), 437-440.

Cotfas, D. (N/A). Measurement of Solar Radiation Calibration of PV cells. Retrieved from https://slidetodoc.com/measurement-of-solar-radiation-calibration-of-pv-cells/

Dondariya, C., Porwal, D., Awasthi, A., Shukla, A. K., Sudhakar, K., S.R, M. M., & Bhimte, A. (2018). Performance simulation of grid-connected rooftop solar PV system for small households: A case study of Ujjain, India. *Energy Reports, 4*, 546-553. doi:https://doi.org/10.1016/j.egyr.2018.08.002

Ebhota, W. S. (2019). Power accessibility, fossil fuel and the exploitation of small hydropower technology in sub-saharan Africa. *International Journal of Sustainable Energy Planning and Management, 19*. doi: https://doi.org/10.5278/ijsepm.2019.19.3

Ebhota, W. S., Eloka-Eboka, A. C., & Inambao, F. L. (2014). *Energy sustainability through domestication of energy technologies in third world countries in Africa*. Paper presented at the Industrial and Commercial Use of Energy (ICUE) 2014 International Conference. https://ieeexplore.ieee.org/document/6904197

Ebhota, W. S., & Inambao, F. L. (2015). *Domestic Turbine Design, Simulation and Manufacturing for Sub-Saharan Africa Energy Sustainability*. Paper presented at the 14th International Conference on Sustainable Energy Technologies – SET 2015, Nottingham, UK.

Ebhota, W. S., & Inambao, F. L. (2017). Facilitating Greater Energy Access in Rural and Remote Areas of Sub-Saharan Africa: Small Hydropower. *Energy & Environment, 28*(3), 316-329. doi:http://journals.sagepub.com/doi/abs/10.1177/0958305X16686448

Ebhota, W. S., & Jen, T.-C. (2018). Efficient Low-cost Materials for Solar energy applications: Roles of nanotechnology *Photovoltaic Materials and Solar Panels* (1 ed.). United Kingdom: IntechOpen.

Ebhota, W. S., & Jen, T.-C. (2018). *Photovoltaic solar energy: potentials and outlooks*. Paper presented at the ASME International Mechanical Engineering Congress and Exposition, Pittsburgh, Pennsylvania, USA. http://dx.doi.org/10.1115/IMECE2018-86991

Ebhota, W. S., & Tabakov, P. Y. (2018). The place of small hydropower electrification scheme in socioeconomic stimulation of Nigeria. *International Journal of Low-Carbon Technologies, 13*(4), cty038-cty038. doi:https://doi.org/10.1093/ijlct/cty038

Ebhota, W. S., & Tabakov, P. Y. (2019). Power Supply and the Place Hydropower in sub-Saharan Africa's Modern Energy System and Socioeconomic Wellbeing. *International Journal of Energy Economics and Policy, 9*(2), 347-363 doi:https://doi.org/10.32479/ijeep.7184

Eiden, T. J. (2014). Nuclear Energy: The Safe, Clean, Cost-Effective Alternative. *The Objective Standard, Fall 2013, 8*(3).

FloodList. (2019a). DR Congo – 600,000 Affected by Floods in 12 Provinces, Says UN. Retrieved from http://floodlist.com/africa/dr-congo-floods-december-2019

FloodList. (2019b). Uganda – More Fatalities After Floods in Central and Eastern Regions. Retrieved from http://floodlist.com/africa/uganda-floods-central-eastern-region-december-2019

Fu, P., & Rich, P. M. (2002). A geometric solar radiation model with applications in agriculture and forestry. *Computers and Electronics in Agriculture, 37*(1), 25-35. doi:https://doi.org/10.1016/S0168-1699(02)00115-1

Fuzen. (2021). List of solar PV design software tools. Retrieved from https://www.fuzen.io/solar-epc/list-of-solar-pv-design-software-tools/

IEA. (2017). *Energy Access Outlook: From Poverty to Prosperity*. Retrieved from Paris, France: http://www.iea.org/publications/freepublications/publication/WEO2017SpecialReport_EnergyAccessOutlook.pdf

Kammen, D. M., & Sunter, D. A. City-Integrated Renewable Energy for Urban Sustainability. Retrieved from https://gspp.berkeley.edu/research/featured/city-integrated-renewable-energy-for-urban-sustainability

Khatib, T., Mohamed, A., & Sopian, K. (2012). A Software Tool for Optimal Sizing of PV Systems in Malaysia. *Modelling and Simulation in Engineering, 2012*, 969248. doi:10.1155/2012/969248

Li, C. (2021). Evaluation of the viability potential of four grid-connected solar photovoltaic power stations in Jiangsu Province, China. *Clean Technologies and Environmental Policy*. doi:10.1007/s10098-021-02111-1

Marion, B., Adelstein, J., Boyle, K., Hayden, H., Hammond, B., Fletcher, T., . . . Townsend, T. (2005, 3-7 Jan. 2005). *Performance parameters for grid-connected PV systems.* Paper presented at the Conference Record of the Thirty-first IEEE Photovoltaic Specialists Conference, 2005.

Nachmany, M., Fankhauser, S., Townshend, M., Collins, T., Landesman, T., Matthews, A., . . . Setzer, J. (2014). The Globe Climate Legislation Study: A Review of Climate Change Legislation in 66 Countries. *Globe International and the*

Grantham Research Institute, London School of Economics, London.

Njoku, H. O., & Omeke, O. M. (2020). Potentials and financial viability of solar photovoltaic power generation in Nigeria for greenhouse gas emissions mitigation. *Clean Technologies and Environmental Policy, 22*(2), 481-492. doi:10.1007/s10098-019-01797-8

NREL. (2016). *Transforming Energy through Science*. Retrieved from National Renewable Energy Laboratory, Office of Energy Efficiency and Renewable Energy, USA:

Park, N. C., Oh, W. W., & Kim, D. H. (2013). Effect of Temperature and Humidity on the Degradation Rate of Multicrystalline Silicon Photovoltaic Module. *International Journal of Photoenergy, 2013*, 925280. doi:10.1155/2013/925280

Rich, P. M., Dubayah, R., Hetrick, W. A., & Saving, S. C. (1994). Using viewshed models to calculate intercepted solar radiation: applications in ecology. *American Society for Photogrammetry and Remote Sensing Technical Papers*, 524-529.

Rinaldi, F., Moghaddampoor, F., Najafi, B., & Marchesi, R. (2021). Economic feasibility analysis and optimization of hybrid renewable energy systems for rural electrification in Peru. *Clean Technologies and Environmental Policy, 23*(3), 731-748. doi:10.1007/s10098-020-01906-y

Roadmap. (2020). Technology-Roadmap: Solar Photovoltaic (PV) Roadmap for Singapore. Retrieved from https://www.nccs.gov.sg/media/publications/technology-roadmap

Roos, C., Nelson, M., & Brockman, K. (2009). Solar Electric System Design, Operation and Installation: An Overview for Builders in the Pacific Northwest. *Washington State University Extension Energy Program*.

Shiva Kumar, B., & Sudhakar, K. (2015). Performance evaluation of 10 MW grid connected solar photovoltaic power plant in India. *Energy Reports, 1*, 184-192. doi:https://doi.org/10.1016/j.egyr.2015.10.001

Shrestha, A. K., Thapa, A., & Gautam, H. (2019). Solar Radiation, Air Temperature, Relative Humidity, and Dew Point Study: Damak, Jhapa, Nepal. *International Journal of Photoenergy, 2019*, 8369231. doi:10.1155/2019/8369231

UN. (2015). *Resolution adopted by the General Assembly on 25 September 2015*. Paper presented at the United Nations New York. http://daccess-ods.un.org/access.nsf/GetFile?OpenAgent&DS=A/RES/70/1&Lang=E&Type=DOC

Weather&Climate. (2021). Climate in Durban (KwaZulu-Natal), South Africa. Retrieved from https://weather-and-climate.com/average-monthly-Rainfall-Temperature-Sunshine,durban,South-Africa

World Energy Council. (2013, 15/01/2018). World Energy Resources: Solar Retrieved from https://www.worldenergy.org/wp-content/uploads/2013/10/WER_2013_8_Solar_revised.pdf

Worlddata.info. (2021). Sunrise and sunset in South Africa. Retrieved from https://www.worlddata.info/africa/south-africa/sunset.php

Supplementary Files

This is a list of supplementary files associated with this preprint. Click to download.

- Graphicabstract.doc